Improving the Community Geodetic Model with GPS and InSAR

Report for SCEC Award #15073
Submitted March 7, 2016

Investigators:

David Sandwell (SIO)
Alejandro Gonzalez-Ortega (CICESE)
Javier Gonzalez (CICESE)
Bridget Smith-Konter (UH)
Yuehua Zeng (USGS)

I. Project Overview

A. Abstract

In the box below, describe the project objectives, methodology, and results obtained and their significance. If this work is a continuation of a multi-year SCEC-funded project, please include major research findings for all previous years in the abstract. (Maximum 250 words.)

One of the priorities of SCEC4 is to investigate *stress transfer from plate motion to crustal faults*. Surface crustal velocities are one of the key boundary conditions needed for developing 3-D stress rate models. The quality and quantity of GPS and InSAR data are increasing rapidly and many groups are developing detailed crustal velocity models. Over the past year we have contributed in two areas.

1) We have collaborated with other SCEC and PBO scientists to develop a time-dependent Community Geodetic Model (CGM) at variable spatial resolution. Murray and Sandwell led a Community Geodetic Model (CGM) Workshop, January 28 – 29, 2016, Pomona, CA. The workshop overview, agenda and participants are provided on a SCEC web site https://www.scec.org/workshops/2016/cgm. The workshop report is in press at SCEC. In 2015 Sandwell assembled secular velocity models from 15 groups. These will form the basis for the secular CGM. In addition, the models will be converted to horizontal strain rate for cross comparisons as well as comparison with SHmax from seismic studies.

2) We worked with CICESE scientists to acquire spatially dense GPS velocities across the Imperial and Cerro Prieto Faults. The preliminary results of the analysis of slip rates and locking depths across these two faults are provided in Figure 1. There is a significant step in velocity across the Imperial Fault of 29 $\pm$ 4 mm/yr with a locking depth of 7.3 km. This rate is somewhat smaller than the slip rate of 35 mm/yr north of the border. More important we find the full plate rate of more than 40 mm/yr is realized between the most distant points across the fault (PJZX – IID2); the sum of the model slip rates is 50 mm/yr.

B. SCEC Annual Science Highlights

Each year, the Science Planning Committee reviews and summarizes SCEC research accomplishments, and presents the results to the SCEC community and funding agencies. Rank (in order of preference) the sections in which you would like your project results to appear. Choose up to 3 working groups from below and re-order them according to your preference ranking.

Tectonic Geodesy
Community Modeling Environment (CME)

C. Exemplary Figure

Select one figure from your project report that best exemplifies the significance of the results. The figure may be used in the SCEC Annual Science Highlights and chosen for the cover of the Annual Meeting Proceedings Volume. In the box below, enter the figure number from the project report, figure caption and figure credits.

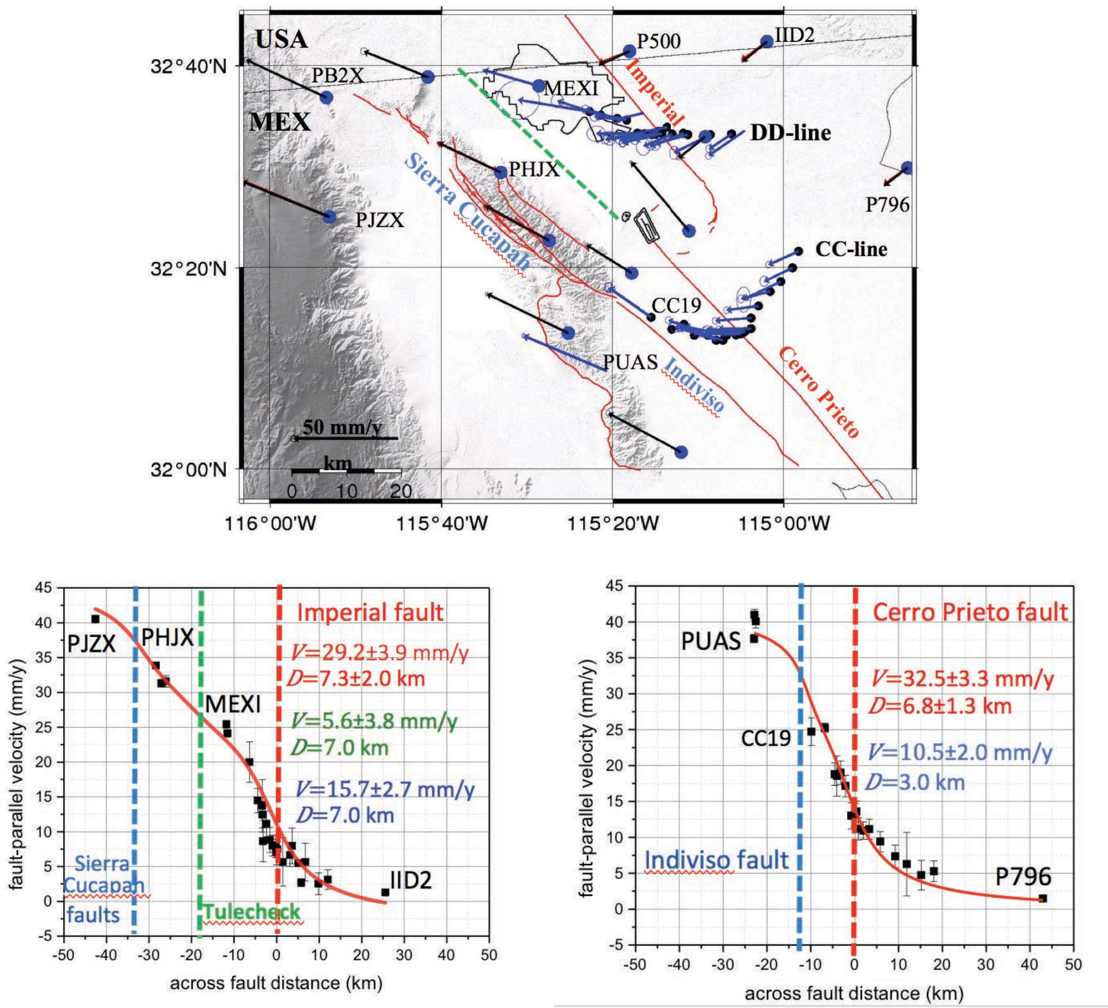

Figure 1. (upper) Location map of active strike-slip faults in Northern Baja California. The Imperial Fault passes through a highly populated area of eastern Mexicali. The Cerro Prieto Fault ends at the geothermal pond of the geothermal power generation plant. Continuous GPS sites are shown as blue dots and campaign GPS monuments are shown as black dots. The velocity vectors are relative to the ITRF. (lower left) Fault-parallel velocity versus distance across the Imperial Fault. The preliminary model has two additional faults to the west to explain the significant changes in velocity. (lower right) Fault-parallel velocity versus distance across the Cerro Prieto Fault. The preliminary model has one additional fault to the west of the Cerro Prieto Fault. We are developing a time-dependent model that includes the postseismic deformation of the El Major-Cucupah earthquake to explain these data.

D. SCEC Science Priorities

In the box below, please list (in rank order) the SCEC priorities this project has achieved. See *https://www.scec.org/research/priorities* for list of SCEC research priorities. *For example: 6a, 6b, 6c*

1d. Development of a Community Geodetic Model (GCM) for California
1e. Combined modeling/inversion studies to interpret GPS and InSAR geodetic results.

E. Intellectual Merit

How does the project contribute to the overall intellectual merit of SCEC? *For example: How does the research contribute to advancing knowledge and understanding in the field and, more specifically, SCEC research objectives? To what extent has the activity developed creative and original concepts?*

The San Andreas Fault System (SAFS) is a natural laboratory for investigating the physics of the earthquake cycle along a major continental transform boundary. Two of the key parameters that can be used for seismic hazard assessment are seismic moment accumulation rate and strain accumulation rate. The GPS component of the Plate Boundary Observatory (PBO) provides accurate vector velocities (< 1 mm/yr accuracy) at a spacing of 10 to 20 km along the SAFS. However, the velocity gradient (strain rate) varies most rapidly within 20 km of the major faults, so strain rate is not well resolved by the GPS data alone. Radar interferometry (InSAR) provides deformation maps at 100 m spatial resolution, although factors such as temporal decorrelation and atmospheric path errors have made it difficult to achieve this full resolution with sufficient precision to improve upon the GPS measurements. The primary focus of our research is to construct high spatial resolution vector surface deformation measurements by combining the high accuracy point measurements provided by PBO GPS data with the high spatial resolution InSAR measurements.

F. Broader Impacts

How does the project contribute to the broader impacts of SCEC as a whole? *For example: How well has the activity promoted or supported teaching, training, and learning at your institution or across SCEC? If your project included a SCEC intern, what was his/her contribution? How has your project broadened the participation of underrepresented groups? To what extent has the project enhanced the infrastructure for research and education (e.g., facilities, instrumentation, networks, and partnerships)? What are some possible benefits of the activity to society?*

These proposed research activities will contribute to the objectives of SCEC by further advancing our understanding of fault system crustal dynamics, earthquake hazards, and data synthesis. The fundamental earthquake science being explored by this research has substantial societal relevance, as earthquake cycle strain rate estimates are poised to help mitigate seismic hazards.

G. Project Publications

All publications and presentations of the work funded must be entered in the SCEC Publications database. Log in at *http://www.scec.org/user/login* and select the Publications button to enter the SCEC Pubications System. Please either (a) update a publication record you previously submitted or (b) add new publication record(s) as needed. If you have any problems, please email *web@scec.org* for assistance.

Tong, X. D.T. Sandwell and B. Smith-Konter, An integral method to estimate the moment accumulation rate on the Creeping Section of the San Andreas Fault, *Geophys. J. Int.,* 203 (1), 48-62, 2015. (SCEC #6197)

Xu, X., X. Tong, D. T. Sandwell, C. Millner, J. F. Dolan, J. Hollingsworth, S. Leprince, F. Ayoub, Refining the shallow slip deficit, *Geophys. J. Int., 203*, 48-62, doi: 10.1093/gji/ggv269, 2015. (SCEC #6198)

II. Technical Report

A. Summary

One of the priorities of SCEC4 is to investigate *stress transfer from plate motion to crustal faults*. Surface crustal velocities are one of the key boundary conditions needed for developing 3-D stress rate models. The quality and quantity of GPS and InSAR data are increasing rapidly and many groups are developing detailed crustal velocity models. Over the past year we have: collaborated with other SCEC and PBO scientists to develop a time-dependent Community Geodetic Model (CGM) at variable spatial resolution; worked with CICESE scientists to acquire spatially dense GPS velocities across the Imperial and Cerro Prieto Faults and; participated in SCEC workshops related to the development of the Community Geodetic Model as well as the Community Stress Model.

1. Collaborate with other SCEC and PBO scientists to develop a time-dependent Community Geodetic Model (CGM) at variable spatial resolution. Work with SCEC community on optimal integration of InSAR and GPS.

Murray and Sandwell led a Community Geodetic Model (CGM) Workshop, January 28 – 29, 2016, Pomona, CA. The workshop overview, agenda and participants are provided on a SCEC web site https://www.scec.org/workshops/2016/cgm . The workshop report is in press at SCEC.

During 2015 we assembled secular velocity models from 15 groups. These will form the basis for the secular CGM. In addition, the models will be converted to horizontal strain rate for cross comparisons as well as comparison with SHmax from seismic studies. We believe the assembly and comparison of existing models results in a "friendly competition" among investigators. The main science driver for this assembly/analysis is to examine the strain partitioning between elastic strain buildup in the near field of the main faults and off-fault inelastic deformation. A previous analysis of strain-rate map produced by 16 different research groups using primarily the same GPS velocity measurements, reveals that modeled strain rate can differ by factors of 5 to 8 times, with the largest differences occurring along the most active faults [Hearn et al., 2010]. The original published strain rate models [Bird, 2009; Freed et al., 2007; Hackl et al., 2009; Kreemer et al., 2009; McCaffrey, 2005; Meade and Hager, 2005a and 2005b; Parsons, 2006; Platt et al., 2008; Platt and Becker, 2010; Shen et al., 1996; Smith-Konter and Sandwell, 2009; Tape et al., 2009] were based on largely the same GPS vector velocity measurements so differences among models reflect differences in interpolating the velocity field between the GPS sites [Hearn et al., 2010].

One of the more interesting outcomes of this preliminary analysis was that the mean strain rate of the 5 "best" models has a very high correlation (0.8) with the background seismicity rate [Petersen et al., 2008]. This very preliminary analysis suggests that, as expected, strain rate provides a proxy for seismicity rate that is worth further research [Shen et al., 2007]. There are a few important differences between the strain rate and the seismicity rate. First the seismicity rate is very low on the eastern side of the study region while the strain rate in this region is not especially low. Second the strain rate is high on the Panamint Valley and Death Valley-Black Mtn faults while the seismicity in that area is low. Are these this differences real or an artifact of the interpolation errors in the strain rate maps? Through our investigation we hope to answer this question.

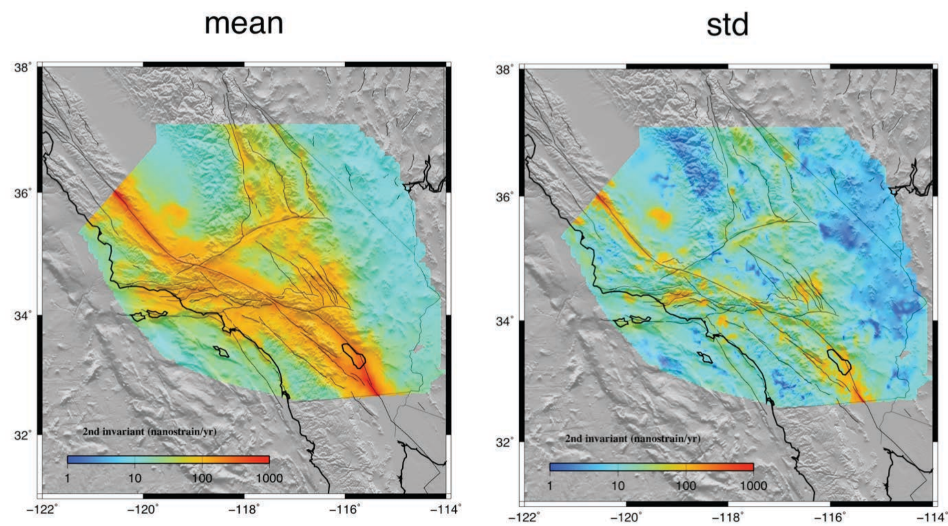

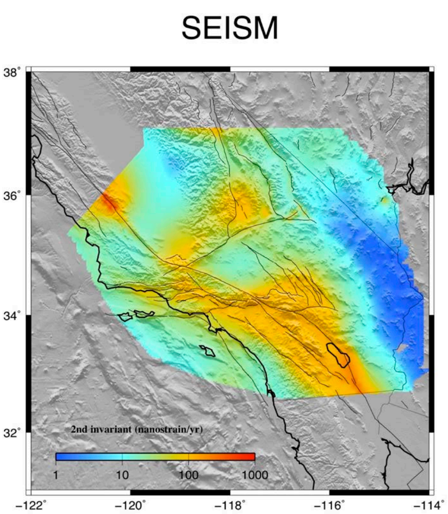

Figure 1. (upper) Mean and standard deviation of strain rate for the 5 "best" of 16 models contributed by the research community. The disagreements among the 5 models, shown as the standard deviation, provides a quantitative measure of what is known and unknown about strain rate. Large strain rate uncertainties of 100 to 300 nanostrain occur within 20 km of the major faults, especially the creeping sections. In addition, several models have strain artifacts along block boundaries and at block intersections. (lower) Background seismicity rate for M 5.0 - 6.5 earthquakes on faults and for random M 5.0 – 7.0 earthquakes that do not occur on faults included in the model [*Petersen et al.,* 2008]. An arbitrary constant of 5.3 is added to the log of the rate to match the strain rate colorbar.

A second science driver for the assembly and analysis of strain rate maps is to better characterize the relationship between the orientation of the maximum compressive strain and the maximum horizontal compressive stress (SHmax) determined from an analysis of earthquake focal mechanisms [Yang and Hauksson, 2013]. The high correlation between these two tensor fields suggests that strain rate maps serve as a proxy for stressing rate and ultimately seismicity rate and orientation. One intriguing aspect of this analysis is that there is an approximate 5 degree rotation between the maximum compressive strain rate and the direction of SHmax (Figure 2).

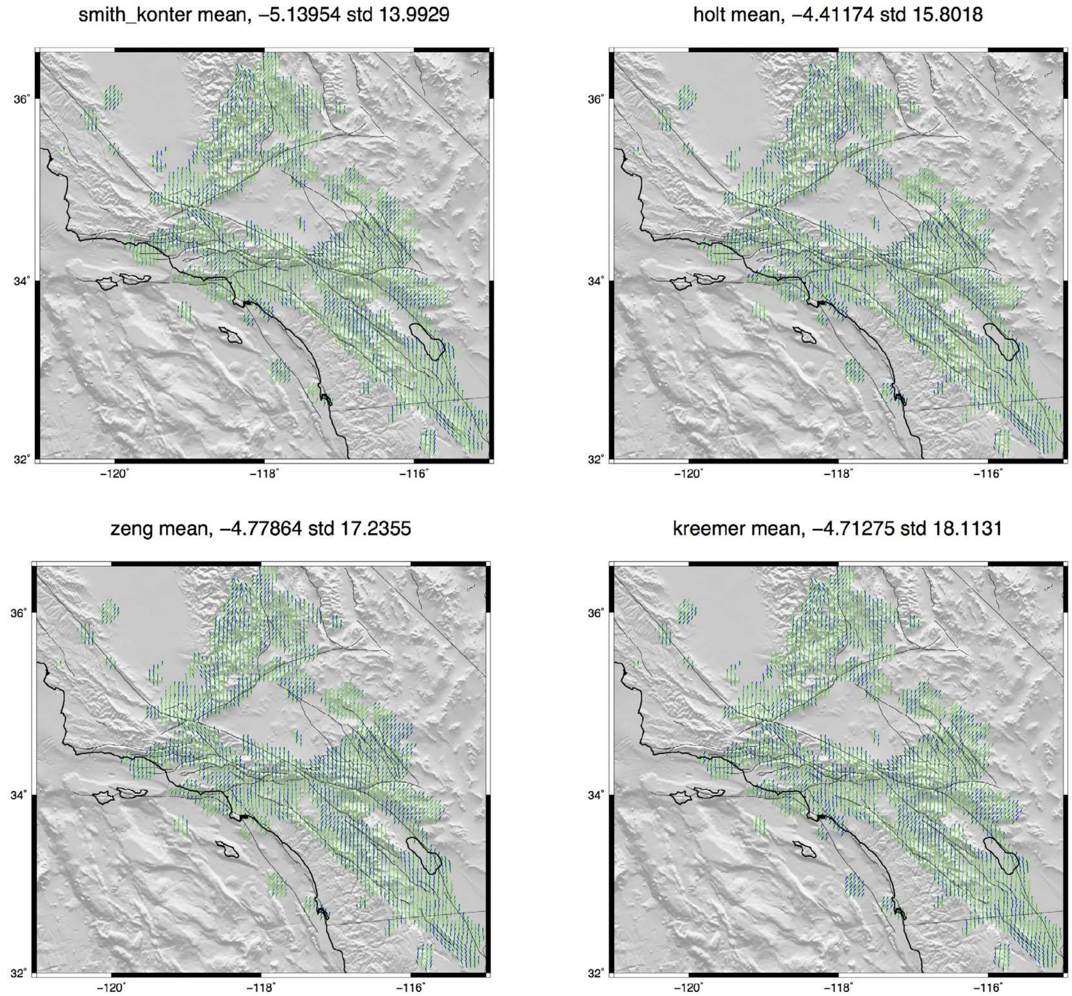

Figure 2. Comparison between the orientation of SHmax (blue) [Yang and Hauksson, 2013] and direction of maximum compression from 4 strain-rate models. There is a good agreement between these two with a typical rms deviation of 15 degrees. More interesting, there is a consistent 5 degree average rotation of the strain field with respect to the SHmax field. We proposed to further explore this comparison with the new compilation.

We are working with Phillip Maechling at SCEC to assemble a new compilation of crustal motion products on the SCEC web site. We have contacted all the authors from the previous compilation and asked whether they still want to have their model evaluated and also asked for an update. The initial assembly is being done on our computer and you can access the compilation at the following ftp location (ftp://topex.ucsd.edu/pub/sandwell/strain/). Table 1 shows the status of the assembly. During 2016 we plan to complete this analysis and web site.

Table 1.

NAME	GPS VEL	INSAR VEL	MODEL VEL	MODEL STRAIN_RATE	PUBLICATION
becker				X	Platt and Becker, 2010
bird	X		X	X	Petersen et al., 2014; Field et al., 2014
hackl			X	X	Hackl, 2009
hammond	X		X		Johnson et al., 2013
holt	X		X	X	Flesch et al., 2000
kreemer	X		X	X	Kreemer et al., 2014
lindsey		X			Lindsey et al., 2014

loveless_mead	X		X		Loveless and Meade, 2011
mccaffrey	X		X	X	McCaffrey et al., 2013
parsons			X	X	Parsons et al., 2006
shen	X		X	X	Shen et al., 2015
smith_konter	X		X	X	Smith-Konter and Sandwell, 2009
tape			X	X	Tape et al., 2009
tong	X	X	X	X	Tong et al., 2013
zeng	X		X	X	Field et al., 2014

2. Collaborate with CICESE scientists to acquire spatially dense GPS velocities across the Imperial and Cerro Prieto Faults and analyze InSAR imagery from WInSAR database.

Over the past six years, using SCEC funds, we (SIO and CICESE) have installed and surveyed GPS arrays across the Imperial and Cerro Prieto Faults to better characterize their moment accumulation rates and thus their seismic potential. The 19 monuments of the DD-line (Figures 3) were deployed in March of 2010 just prior to the El Mayor-Cucapah event on April 4 and they were first surveyed in May 2010 although these initial data are largely contaminated by the postseismic signal of the earthquake. The DD-line was resurveyed in early 2012, 2014, and 2015. The 17 monuments of the CC-line were deployed and surveyed in early 2011. The CC-line was resurveyed in early 2013 and 2015. The total aperture and spacing of the monuments is optimal for estimating locking depth.

The preliminary results of the analysis of slip rates and locking depths across these two faults are provided in Figure 3. There is a significant step in velocity across the Imperial Fault of 29 + 4 mm/yr with a locking depth of 7.3 km. This rate is somewhat smaller than the slip rate of 35 mm/yr north of the border. More important we find the full plate rate of more than 40 mm/yr is realized between the most distant points across the fault (PJZX – IID2); the sum of the model slip rates is 50 mm/yr. Modeling the wider GPS array requires significant slip on additional faults (Tulecheck and Sierra Cucupah). One complicating factor is that these measurements are effected by the postseismic deformation following the El Mayor-Cucapah event in April 2010 [Gonzalez-Ortega et al., 2014]. We find a similar slip-rate discrepancy with the Cerro Prieto Fault where our preliminary estimate of slip rate of 33+3 mm/yr is significantly less than the published rates of 40 and 42 mm/yr.

During the final year of SCEC 4 we plan to resurvey both the DD and CC lines and also install additional campaign GPS monuments to the west of the main faults so that in future years we will be able to better characterize the slip rates on these poorly mapped faults. In addition we will more carefully examine the available InSAR data from Envisat as well as the new more frequent acquisitions from Sentinel-1A and ALOS-2. By the end of SCEC 4 we propose to have a much-improved understanding of the deformation associated with the faults in Northern Baja California.

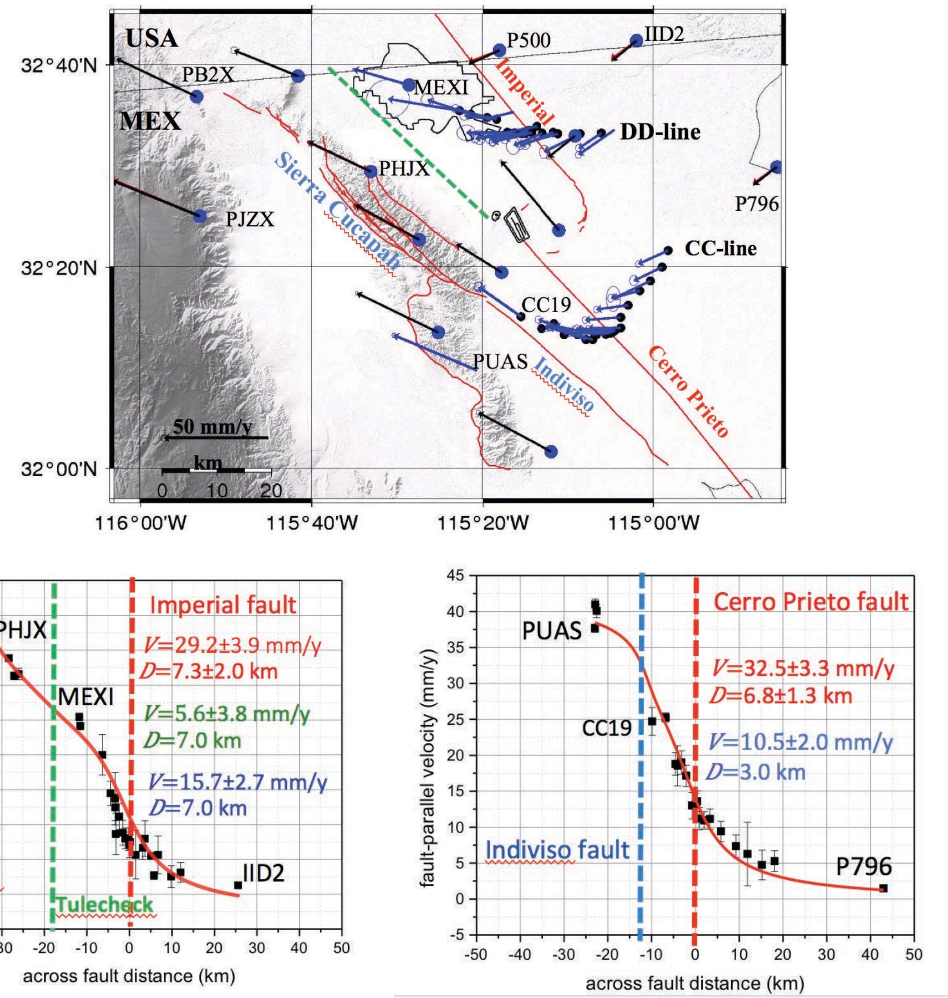

Figure 3. (upper) Location map of active strike-slip faults in Northern Baja California. The Imperial Fault passes through a highly populated area of eastern Mexicali. The Cerro Prieto Fault ends at the geothermal pond of the geothermal power generation plant. Continuous GPS sites are shown as blue dots and campaign GPS monuments are shown as black dots. The velocity vectors are relative to the ITRF. (lower left) Fault-parallel velocity versus distance across the Imperial Fault. The preliminary model has two additional faults to the west to explain the significant changes in velocity. (lower right) Fault-parallel velocity versus distance across the Cerro Prieto Fault. The preliminary model has one additional fault to the west of the Cerro Prieto Fault. We are developing a time-dependent model that includes the postseismic deformation of the El Major-Cucupah earthquake to explain these data.

B. References

Bennett, R., W. Rodi, and R. Reilinger, Global Positioning System constraints on fault slip rates in southern California and northern Baja, Mexico, J. Geophys. Res., 101, B10, 21943-21960, 1996.

Bird, P., Long-term fault slip rates, distributed deformation rates, and forecast of seismicity in the western United States from joint fitting of community geologic, geodetic, and stress-direction datasets, J. Geophys. Res., 114, B11403, doi:10.1029/2009JB006317, 2009.

Field, E. H., Arrowsmith, R. J., Biasi, G. P., Bird, P., Dawson, T. E., Felzer, K. R., ... & Zeng, Y. (2014). Uniform California Earthquake Rupture Forecast, Version 3 (UCERF3)–The Time‐Independent Model. Bulletin of the Seismological Society of America, 104(3), 1122-1180.

Flesch, L. M., Holt, W. E., Haines, A. J., & Shen-Tu, B. (2000). Dynamics of the Pacific-North American plate boundary in the western United States. Science, 287(5454), 834-836.

Freed, A. M., S. T. Ali, and R. Burgmann, Evolution of stress in Southern California for the past 200 years from coseismic, postseismic and interseismic stress changes, Geophys. J. Int.,169, p. 1164-1179, 2007.

González-Ortega, J. A., Y. Fialko, D. Sandwell, F. A. Nava Pichardo, J. Fletcher Mackrain, J. J. Gonzalez Garcia, B. Lipovski , M. Floyd y G. Funning. El Mayor-Cucapah (Mw 7.2) earthquake: Early near-field postseismic deformation from InSAR and GPS observations. Journal of Geophysical Research. Solid Earth. 119(2): 1482-1497. 2014.

Hackl, M., R. Malservaisi, and S. Wdowinski, Strain pattern from dense GPS networks, Nat. Hazards Earth Syst., 9., 1177-1187, 2009.

Hauksson, E., and D. Sandwell (2013), Comparison of SHmax orientations from stress inversions of focal mechanisms with 17 different strain models determined from GPS data in southern California: Contribution to the SCEC stress model, SCEC Annual Meeting, poster 087.

Hearn, E., K. Johnson, D. Sandwell, and W. Thatcher, SCEC UCERF workshop report: http://www.scec.org/workshops/2010/gps-ucerf3/FinalReport_GPS-UCERF3Workshop.pdf, 2010.

Johnson, K., P. Bird, Y. Zeng, W. Thatcher, T. Dawson, R. Weldon, R. McCaffrey, W.C. Hammond, J. Bormann, T. Herring, 2013, Geodetically-derived deformation models for UCERF3, report for the Working Group On California Earthquake Probabilities, available at http://wgcep.org.

Kreemer, C., G. Blewitt, W. C. Hammond, and H. P. Plang, A high-resolution strain rate tensor model for the western U. S., EarthScope National Meeting 2009, Boise, ID, 2009.

Kreemer, C., G. Blewitt, and E. C. Klein (2014), A geodetic plate motion and Global Strain Rate Model, Geochem. Geophys. Geosyst., 15, 3849–3889, doi:10.1002/2014GC005407.

Lindsey, E. O., Fialko, Y., Bock, Y., Sandwell, D. T., & Bilham, R. (2014). Localized and distributed creep along the southern San Andreas Fault. Journal of Geophysical Research: Solid Earth, 119(10), 7909-7922.

Loveless, J. P., & Meade, B. J. (2011). Stress modulation on the San Andreas fault by interseismic fault system interactions. Geology, 39(11), 1035-1038.

McCaffrey, R., Block kinematics of the Pacific–North America plate boundary in the southwestern United States from inversion of GPS, seismological, and geologic data, J. Geophys. Res., 110, B07401, doi:10.1029/2004JB003307, 2005.

McCaffrey, R., King, R. W., Payne, S. J., & Lancaster, M. (2013). Active tectonics of northwestern US inferred from GPS‐derived surface velocities. Journal of Geophysical Research: Solid Earth, 118(2), 709-723.

Meade, B.J., and B.H. Hager, Block models of crustal motion in southern California constrained by GPS measurements, J. Geophys. Res., 110, doi:10.1029/2004JB003209, 2005a.

Meade, B.J., and B.H. Hager, Spatial localization of moment deficits in southern California, J. Geophys. Res., 110, doi:10.1029/2004JB003331, 2005b.

Parsons, T., Tectonic stressing in California modeled from GPS observations, J. Geophys. Res. 111, doi:10.1029/2005JB003946, 2006.

Parsons, T., K.M. Johnson, P. Bird, J.M. Bormann, T.E. Dawson, E.H. Field, W.C. Hammond, T.A. Herring, R. McCaffrey, Z.-K. Shen, W.R. Thatcher, R.J. Weldon and Y. Zheng, 2013, Appendix C- Deformation models for UCERF3, USGS Open-File Report, v. 2013-1165, 66 pp., http://pubs.usgs.gov/of/2013/1165/pdf/ofr2013-1165_appendixC.pdf.

Petersen, M. D., Mueller, C. S., Frankel, A. D., & Zeng, Y. Appendix J: Spatial Seismicity Rates and Maximum Magnitudes for Background Earthquakes, USGS Open File Report 2007-1437J, 2008.

Petersen, M. D., Y. Zeng, K. M. Haller, R. McCaffrey, W. C. Hammond, P. Bird, M. Moschetti, Z. Shen, J. Bormann, and W. Thatcher [2014] Geodesy- and geology-based slip-rate models for the Western United States (excluding California) national seismic hazard maps, U.S. Geol. Surv. Open-File Rep., 2013-1293, 38 pages doi.org/10.3133/ofr20131293.

Platt J. P. and T. W. Becker, Where is the real transform boundary in California?, Geochem. Geophys. Geosyst., 11, Q06012, doi:10.1029/2010GC003060, 2010.

Platt, J. P., B. Kaus, and T. Becker, The mechanics of continental transforms: An alternative approach with applications to the San Andreas system and the tectonics of California, Earth Planet. Sci. Lett., v. 274, p. 380-391, 2008.

Shen, Z.-K., D. Jackson, and B. Ge, Crustal deformation across and beyond the Los Angeles Basin from geodetic measurements, J. Geophys. Res., 101, 27957–27980, 1996.

Shen, Z. K., Jackson, D. D., & Kagan, Y. Y. (2007). Implications of geodetic strain rate for future earthquakes, with a five-year forecast of M5 earthquakes in southern California. Seismological Research Letters, 78(1), 116-120.

Shen, Z. K., Wang, M., Zeng, Y., & Wang, F. (2015). Optimal interpolation of spatially discretized geodetic data. Bulletin of the Seismological Society of America.

Smith-Konter, B., D. T. Sandwell, Stress evolution of the San Andreas Fault System: recurrence interval versus locking depth, Geophys. Res., Lett., 35, L13304, doi:10.1029/2009GL037235, 2009.

Tape, C., P. Muse, M. Simons, D. Dong, and F. Webb, Multiscale estimation of GPS velocity fields, Geophys. J. Int., 179, 945-971, 2009.

Tong, X., D. T. Sandwell, and B. Smith-Konter (2013), High-resolution interseismic velocity data along the San Andreas Fault from GPS and InSAR, J. Geophys. Res.; Solid Earth, 118, doi:10.1029/2012JB009442.

Yang, W., and E. Hauksson (2013), The tectonic crustal stress field and style of faulting along the Pacific North America Plate boundary in Southern California, Geophys. J. Int., 194, doi:10.1093/gji/ggt113.